(For submission to JGR Planets, 01 September 1997)

AMMONIA ABUNDANCE AT THE GALILEO PROBE SITE DERIVED FROM ABSORPTION OF THE RADIO SIGNAL

W. M. Folkner and R. Woo

Jet Propulsion Laboratory
California Institute of Technology
Pasadena, California 91109

Abstract

The radio signal from the Galileo probe to the orbiter experienced attenuation due to ammonia in Jupiter's atmosphere during the probe descent. A profile of the ammonia content as a function of depth in the atmosphere has been derived from the measurements of the attenuation. The ammonia content is consistent with solar abundance at the top of the atmosphere, rising to 3.3 times that amount at pressure greater than 10 bar.

Introduction

The Galileo probe used two radio channels transmitting at 1387 MHz to send its engineering and science data to the orbiter. The amplitude of the signal received at the orbiter was sampled at a high rate **(46 ms)** in order 10 study scintillation, turbulence, and refrac[ivc-index fluctuations in Jupiter's atmosphere. Similar measurements were made with the Pioneer Venus probes (Woo et al, 1979). The complicated motion of the probe suspended under its parachute during the descent introduced systematic variability in the same variability as the expected scintillation, making it impossible to separate the scintillations from changes in amplitude caused by changes in the probe orientation.

However, slowly varying amplitude changes could be reliably measured, Thus measurements of the amplitude of the probe radio signal allowed the investigation of some constituents of Jupiter's atmosphere that attenuated the signal, Clouds formed of water-anmonia droplets would be expected to sharply attenuate the signal if the probe had descended through them]. No such **sharp drops in** signal **amplitude were** observed, consistent with other probe experiments that indicated the absence of clouds at the probe site (Ragent et al., 1996; Sromovsky et al. 1996). The only other atmospheric constituent expected to cause significant attenuation of the probe signal is ammonia. The observed attenuation and the inferred profile of ammonia content in Jupiter's atmosphere are given below.

Experiment description

The received radio signal power depended on a number of instrumental and geometric parameters, The geometry of the radio link is shown in Figure 1. The probe moved faster in longitude than the orbiter during the descent, with the orbiter and the probe at the same longitude about 17 minutes into the descent. 'There was about 2.2 degree difference in the probe and orbiter latitudes.

The power received by the orbiter, P_R, is given by

$$P_R = G_A G_R G_S G_T P_T \qquad (1)$$

where P_T is the power transmitted, G_T is transmitting antenna gain, G_S is the 'space loss' due to the distance between the probe and orbiter, G_R is the receiving antenna gain, and G_A is the loss due to atmospheric absorption. Each term is described below. Most quantities are given as functions of time past entry, where the time of entry was fixed by the time the probe was 450 km above the 1 bar reference level. The probe pressure and temperature were measured on the probe (Seiff et al. 1996) and the pressure versus time past entry is shown in Figure 2.

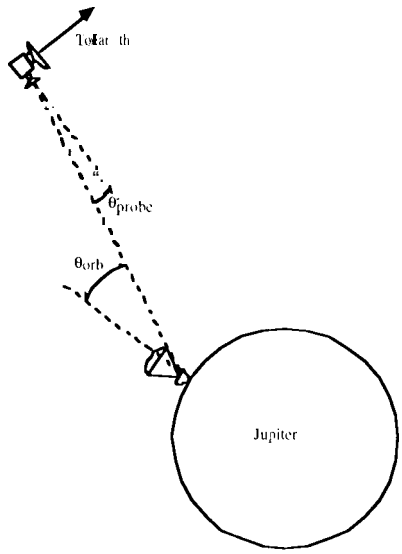

Figure 1. Geometry of the probe-orbiter radio link.

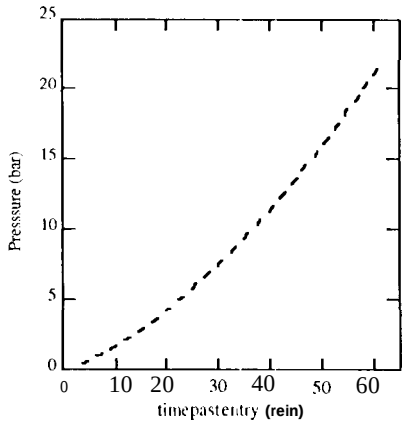

Figure 2. Pressure at probe versus time past entry.

The probe had two radio channels, one M-circular polarized at 1387.0 MHz and one right-circular polarized at 1387.1 Ml Iz. The power transmitted by each channel was monitored on the probe and the power measurements transmitted to the orbiter as part of the telemetry stream. Figure 3 shows the measured transmitted power for each channel over the probe descent. Probe transmission began about 1 90 seconds past entry, and the orbiter receiver locked about 30 seconds later. As the probe descended the temperature of the electronics changed more than had been expected before flight. Both transmitters experienced difficulties about 45 minutes past entry, when the surrounding pressure was about 14 bar and the ambient temperature was 370 K, The LCP transmitter experienced a sharp drop in power followed by a gradual degradation, while the RCP channel failed abruptly.

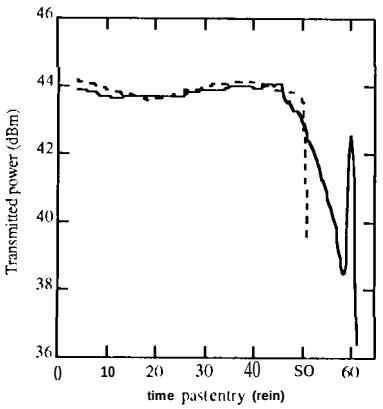

Figure 3. Transmitted power from the probe LCP (solid line) and RCP (dashed line) channels during probe descent.

Both channels were fed to an antenna fixed to the top of the probe, pointing through the parachute and roughly towards the orbiter. The probe antenna was a crossed-dipole with a half-power beam width of 56 degrees. The probe beam pattern was modified by the ground plane provided by the top of the probe housing. The antenna was offset from the center axis by about 20 cm, so some azimuthal asymmetry in probe antenna gain was expected. As the apparent position of the orbiter changed during the descent, the angle between the average antenna axis (local vertical) and the direction to the orbiter varied, The resulting probe antenna gain is shown in Figure 4.

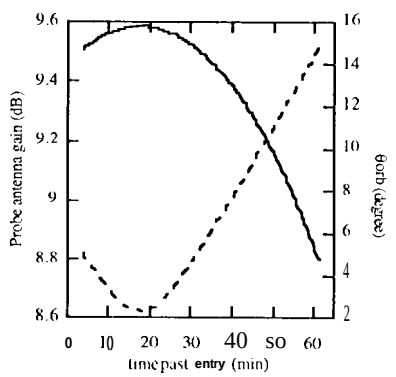

Figure 5. Probe-orbiter distance (solid line) and the resulting space loss (dashed line) during the probe descent.

The distance between the pmbc and orbiter increased throughout the probe descent, The 'space loss' of the signal is given by

$$G_s = \lambda^2 / (4\pi r)^2 \qquad (2)$$

where λ is the radio wavelength and r is the distance between the probe and the orbiter. Figure 5 shows the space loss based on the reconstructed probe and orbiter trajectories.

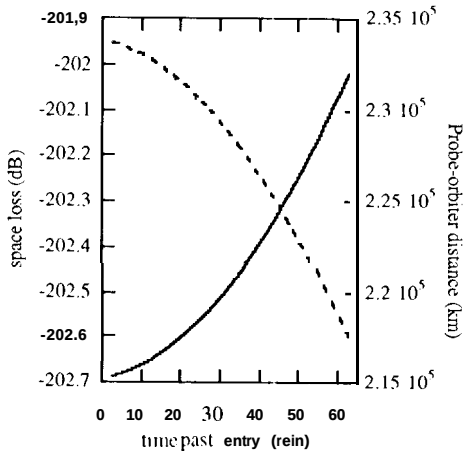

Figure 5. Probe-orbiter distance (solid line) and the resulting space loss (dashed line) during the probe descent.

The orbiter received both probe radio channels through a 1.1 m diameter parabolic antenna, with a half-power beam width of 12,6 degrees. The orbiter antenna pointing was adjusted several times during the probe descent to improve the radio iink performance. The pointing actuator resolution was -0.s degree. "1'here was limited telemetry from the orbiter to indicate how well the planned pointing sequence was performed. The uncertainty in the pointing was estimated to be 2.1 degree (3σ) (Neff 1994). The nominal pointing angle and receiver antenna gain are shown in Figure 6. The times when the antenna was re-pointed can be seen in the received power measurements. After removal of the nominal receiver antenna gain noticeable discontinuities remained in the received power. A constant pointing offset of 0.5 degree was estimated from the data to remove the observed discontinuities.

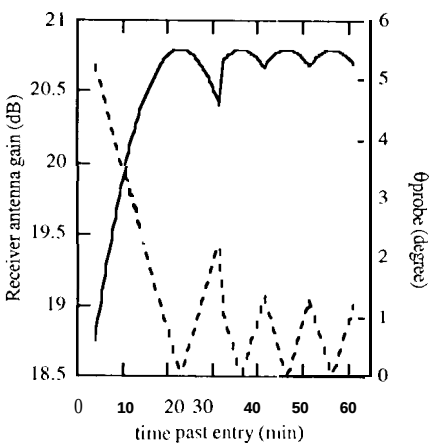

Figure 6. 0~-biter antenna pointing angle and gain during probe descent.

The received power measurements Were made at the output of the telemetry receiver and stored on the orbiter's tape recorder. The received power measurements were then rel ayed to Earth. Not all of the received power measurements were successfully transmitted, leaving one gap of several minutes and a fcw shorter gaps. Differences in the probe and orbiter reference oscillators, and changes caused by Doppler shifts, caused slow variations in the received power measurements. These were removed by estimating the difference in the clock rates from the signatures in the power data (Linkchorst 1996). Several shorter period signatures were also observed in the power measurements, as can been seen in a sample of the data shown in Figure 7. I'here were (typically) two quasi-periodic signatures. One is thought to be to due to the rotation of the probe about the axis connecting the probe to the parachute. The variation in power induced by this rotation was caused by azimuthal asymmetry of the probe antenna pattern. The other major signature seen in the amplitude data was probably caused by the pendulum motion of the probe swinging on its tether below the parachute. Figure 8 shows a series of power spectra formed from two-minute portions of the amplitude data. The amplitude of the variation duc to rotation diminished as the angle between the antenna axis and the direction to the probe decreased, since the probe antenna pattern was more symmetric nearer the antenna axis. The period associated with the probe rotation was initially -6 s, slowing to -14 s 20 minutes after entry and ~50 s at the end of the probe lifetime. The period associated with the probe swinging was about 4 s, with some variation as a function of pressure. A signature period half that of the 'swinging' period is also sometime evident. The swinging period was slightly faster than tbc 4,9s calculated based on simple pendulum motion of the probe suspended by a tether of length ~13.9 m (Stiff et al. 1996),

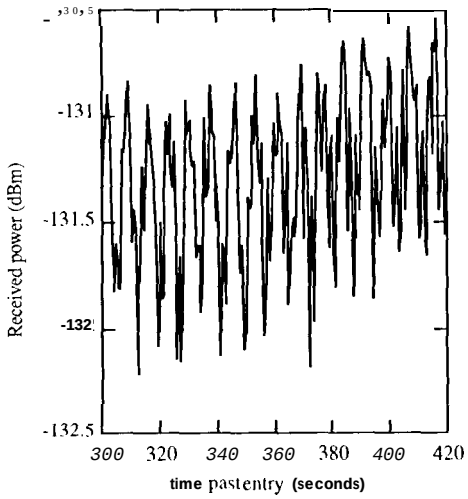

Figure 7. Observed time dependence of the amplitude of the Galileo probe radio signal as received by the orbiter. Each point represents an average of 100 samples taken at 46 ms intervals.

Figure 9 shows the full history of the received power measurements, using averages over 20 s of samples to remove the quasi-periodic signatures. A constant oft'set is evident between the RCP and LCP received power. This could be due to a number of instrumental effects, such as an uncalibrated cable insertion loss between the receiver antenna and the amplifier. A constant loss does not affect the derived atmospheric absorption, assuming that there is effectively no absorption loss at the top of tbc atmosphere at the beginning of the probe descent.

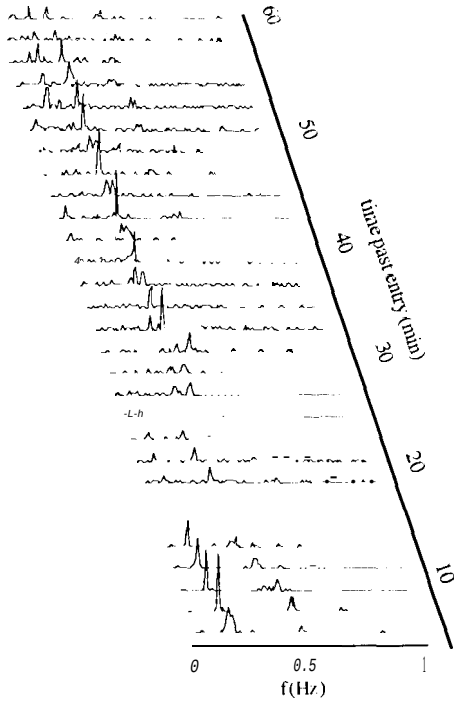

Figure 8. Series of power spectra of the amplitude of tbc Galileo probe radio signal as received by the orbiter. Each spectrum was formed from 2 minutes of amplitude data.

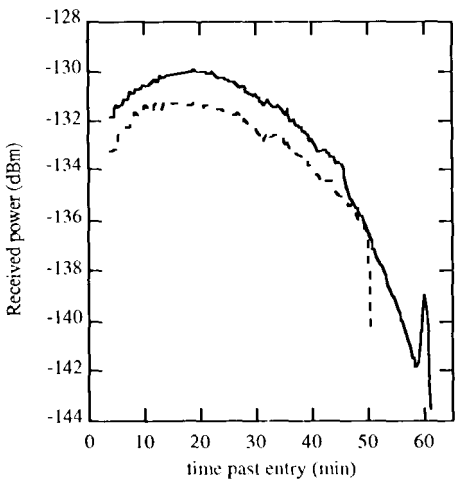

Figure 9. Power received by the orbiter for the LCP(solid line) and RCP (dashed line) channels. Each point represents an average of 400 samples at 46 ms intervals.

Results

The atmospheric absorption of the probe signal, derived by subtracting the known effects from the received power, is shown in Figure10. A constant offset has been added to each channel to give no attenuation at the beginning of the probe descent. The two channels agree well until about 45 minutes past entry, when the pressure was about 14 bar. Shortly after that tbc LCP transmitter degraded and the RCP transmitter failed. At the end of the LCP transmission there is a sharp dip and rise similar to the measured transmitted power (Figure 3). This implies that the measurements of the transmitted power were inaccurate at that time, possibly due to the measurement electronics temperature

being too high. Earlier, the derived LCP attenuation started to flatten out, implying a decrease to zero in atmospheric ammonia. We consider the data past the point where the two channels begin to disagree to be unreliable,

The derived atmospheric attenuation shows no sharp features attributable to clouds. The only significantly absorbing constituent is thought to be ammonia. The absorption expected from ammonia al a constant mole fraction of 0,00022 (solar abundance) is also shown in Figure 10. The absorption coefficient α is calculated by (Rosenkranz 1993)

$$\alpha = n\sum_{J} S_j(T)\,F(\nu,\nu_i) \qquad (3)$$

where n is the number density of ammonia molecules, 7 is the temperature, v is the transmitted radio frequency, and the summation is over molecular resonances with line intensities S,, resonance frequencies v, and shape factors F, I'hc resonance line parameters are given by Poynter and Kakar (1975). The shape factors for ammonia in Jupiter's atmosphere arc dependent on the pressure, temperature, and the helium and ammonia mole fractions (Joiner and Steffes 1991). The helium mole fraction was taken to be 0.136 (von Zahn and Hunten, 1996; Niemann et al. 1996).

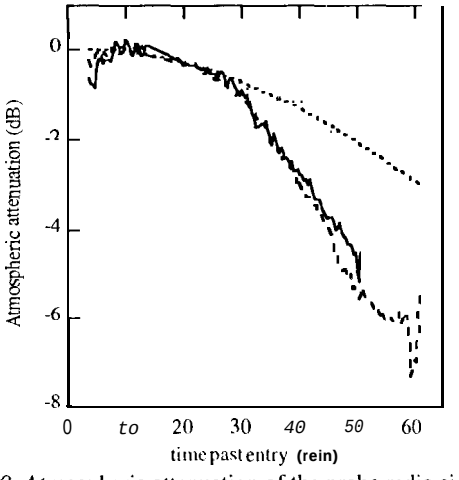

Figure 10. Atmospheric attenuation of the probe radio signal for the RCP (solid line) and LCP (dashed line) channels. The attenuation expected from ammonia at solar abundance is also shown (dot(cd line).

The observed attenuation clearly exceeds the nominal level at about 30 minutes past entry, when the pressure was about 7 bar. There is no data for pressures below 0.4 bar, and little observed attenuation for pressures below 4 bar. Starting at the beginning of probe descent, the amount of ammonia for each time was determined by solving for the number density n to get the observed attenuation from the previous time. Figure 11 shows the derived ammonia mole fraction versus pressure. The uncertainty in the ammonia abundance is due to noise in the power measurements, uncertainties in the receiver antenna pointing, anti motions of the probe,

For pressures below 4 bar the observed ammonia abundance is less than solar. The abundance is not as small as inferred from the net flux radiometer (Sromovsky et al. 1986), though our uncertainties could encompass the difference. The amount of ammonia is seen to increase with pressure up to about 3.3 times solar at a pressure of IO bar, This increase with depth is similar to the increase in the abundance of water and hydrogen sulfide given by the probe's mass spectrometer (Niemann et al, 1996, Mahaffy 1996).

Earlier, Voyager occultation experiments (Lindal et al. 1981) and microwave spectra of Jupiter (De Pater and Massie 1989; DePater 1990; DePater and Mitchell 1993) indicated less than solar ammonia abundance for pressures below 1 bar. The microwave spectra indicated more than solar abundance of ammonia at pressures greater than 1 bar averaged over the surface of Jupiter. The depletion in ammonia for pressures below 4 bar, and the increase for pressures above 4 bar, maybe due to a down draft at the probe site (Atreya et al. 1996; Showman and Ingersoll, 1997).

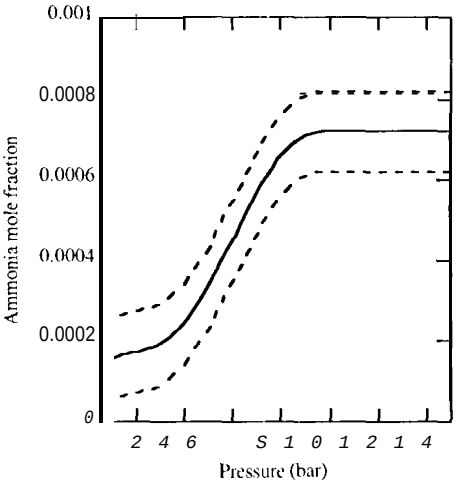

Figure 11. Retrieved ammonia versus pressure (solid line). The dashed lines represent the uncertainties in the retrieval.

Acknowledgment

We wouldlike to thank the Galileo probe project personnel, especially Terry Grant, and Hughes Research Lab personnel, especially Fred Linkehorst, Dan Carlock, and Pete Garriga, for their assistance in processing the probe amplitude data, We also thank Glenn Orton and the Galileo probe science team for helpful discussions. The research described in this paper was, in part, carried out by the Jet Propulsion Laboratory, California Institute of Technology, under a contract with the National Aeronautics and Space Administration.

References

Atreya, S., M. }[. Wong, T. Owen, H. Niemann, and P. Mahaffy, Chemistry and clouds of tbc atmosphere of Jupiter: a Galileo perspective, in *The Three Galileos: The Man, the Spacecraft, the Telescope*, (J. Rahc, C. Barbieri, I'. Johnson, A. Sohu, eds.), Kluwer Academic, Dordrecht, 1996.

DePater, I. and S. T. Massie, Models of the millimeter-centimeter spectra of the giant planets, Icarus, 62, 143-171, 1985.

De Pater, I, A comparison no the deep atmospheres so the giant planets, Advances in Space Research, 10, 79-S7, 1990

Joiner J., and P. G. Steffes, Modeling of Jupiter's millimeter wave emission utilizing laboratory measurements of ammonia opacity, JGR, 96, 17463-17470, 1991.

Lindal, G. F., et al., The atmosphere of Jupiter: an analysis of the Voyager radio occultation measurements, JGR, 86, A 10, 1981.

Linkchorst, F. in Galileo Probe Mission Operations Final Report, Hughes Spacecraft Co. Report HSC 960892, 1996.

Mahaffy, P., recent calibration studies of the Galileo probe neutral mass spectrometer, Eos (fall sup.), 77, F438, 1996.

Neff, J. (cd,). Galileo Probe-Orbiter Relay Link Integration Report, JPL Pub. D-1038 Rev. C, Jet Propulsion Laboratory, California Institute of Technology, 1994.

Niemann, H. B. et al., The Galileo probe mass spectrometer: composition of Jupiter's atmosphere, Science, 272, 846, 1996.

Poynter, R. 1.., and R. K. Kakar, The microwave frequencies, line parameters, and spectral constants for 14NH3, Astrophys. Sup., 29, 87-96, 1975.

Ragent, B., D. S. Colburn, P. Avrin, and K. A. Rages, Results of the Galileo probe nephelometer experiment, Scicncc, 272, 854, 1996,

Stiff A. D., et al., Structure of the atmosphere of Jupiter: Galileo probe measurements, Science, 272, 844, 1996

Sromovsky, L. et al., Solar and thermal radiation in Jupiter's atmosphere: initial results of the Galileo probe net flux radiometer, Science, 272, 851, 1996.

von Zahn, U., and D. M. Hunten, The helium mass fraction in Jupiter's atmosphere, Science 272, 849, 1996.

Woo, R., J. W. Armstrong, and W. B. Kendall, Measurements of turbulence in the Venus atmosphere deduced from Pioneer Venus multiprobe radio scintillations, Science, 205, 87-89.1979.